Compensation of Solenoid Effects at the TESLA Interaction Point

A Wolski
Daresbury Laboratory

Abstract

To achieve high luminosity, the target vertical beam size at the TESLA interaction point is 5 nm. The long solenoid encompassing the detector introduces coupling effects that increase the vertical beam size. In the case that the last quadrupole of the final focus lies inside the solenoid field, the increase in vertical beam size is by as much as two orders of magnitude. In this note, we describe the compensation of the coupling effects using two skew quadrupoles at selected points along the final telescope.

1. Introduction

One of the effects of a solenoid field in a high-energy beam line is to introduce strong coupling between the horizontal and vertical motion of particles travelling along the beam line. This is a concern for a linear collider such as TESLA, where the vertical beam size is much less than the horizontal, and coupling from the detector solenoid at the interaction point will significantly reduce the luminosity. However, it can readily be shown that, with certain approximations, as long as the solenoid and its fringe field are contained within the final drift to the interaction point, coupling from the fringe field actually cancels the coupling from the main solenoid field. However, this is true only for particles travelling directly to the interaction point, and is a good approximation for TESLA where there is no crossing angle and a large beam convergence to the IP.

If a long solenoid is required, that will extend over the last quadrupole of the final focus, then deflection of particle trajectories inside the solenoid destroys the cancellation between the fringe and main fields, and a round beam results. If the IP parameters are fairly relaxed, then sufficient cancellation of the coupling can be achieved by positioning a single skew quadrupole at an appropriate phase with respect to the solenoid. In the case of the parameters for use in the TESLA TDR, however, which demand very small vertical beam size, then a second skew quadrupole is required to reach the required values. As we shall see, the presence of a second skew quadrupole could make it difficult in practice to optimise the strengths of the magnets to achieve the minimum beam size. This is an issue that we do not consider in detail, and only outline proposals for solutions to the problem.

A further concern is the effect of alignment of the solenoid field on the quality of the correction. In principle, rotation of the solenoid field around a horizontal or vertical axis is not expected to introduce any significant new effects, and we expect to be able to counteract the alignment effects by pragmatic tuning of the skew quadrupoles. However, it is still necessary to investigate the sensitivity of the beam size, and the required settings of the skew quadrupoles, to the alignment of the solenoid, and hence derive allowed tolerances on the positioning of the solenoid from beam dynamics considerations.

2. Dynamics in a Solenoid with a (Hard) Fringe Field

We assume that the field inside the solenoid is perfectly uniform and aligned to the z-axis of particle motion. In this case it is clear that a particle entering the solenoid a distance x_0 from the design beam axis, and travelling directly a distance l to the interaction point (see Figure 1), will receive a vertical kick from the main solenoid field:

$$\Delta p_y\big|_{\text{main}} = -eB_s x_0$$

where e is the magnitude of the electron charge, and B_s the strength of the solenoid field, assumed to be in the z direction. Similarly there is a horizontal kick from a vertical offset from the axis:

$$\Delta p_x\big|_{\text{main}} = eB_s y_0$$

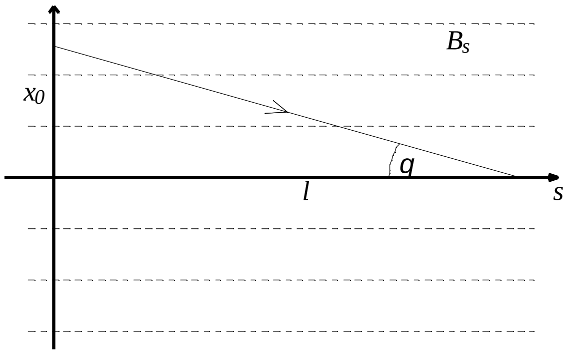

Figure 1
Particle trajectory in the solenoid main field. The particle receives a kick perpendicular to the $x-s$ axes proportional to x_0, the horizontal distance from the s axis on entering the field.

If we now consider the fringe field of the solenoid, we may model this to a first approximation as a flat (i.e. lying entirely in the $x-y$ plane) radial field. Thinking in terms of the field lines exiting the end of the solenoid, the strength of the fringe field must increase linearly with distance from the axis, up to the radius of the solenoid itself. We then find:

$$\Delta p_y\big|_{\text{fringe}} = eB_s x_0$$
$$\Delta p_x\big|_{\text{fringe}} = -eB_s y_0$$

Clearly, the kicks from the fringe field in this approximation exactly cancel the kicks from the main field. To first order, therefore, we expect that there will be no coupling for a beam highly focused on the interaction point.

A critical assumption in the above is that each particle travels directly to the interaction point, starting from a given point off-axis at the entrance to the solenoid. If there is a quadrupole magnet placed inside the solenoid field, this assumption is no longer valid, and the coupling effects of the fringe and main fields must be considered separately. The simplest approach, valid for linear effects of the system we are considering, is to use transfer matrices to investigate the mapping from the input to the final telescope to the interaction point, with and without the solenoid and/or skew quadrupoles.

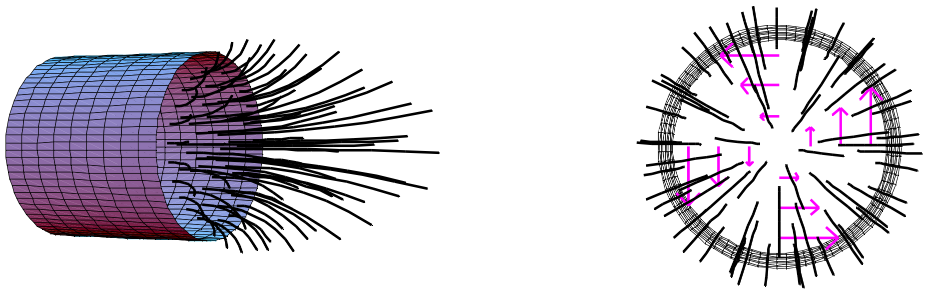

Figure 2
Solenoid fringe field. In a hard fringe approximation, the field increases linearly from the axis. Thus the coupling kicks, represented by arrows in the right hand diagram, also increase linearly.

3. Final Focus Optics and Transfer Maps

The optics used for the present investigations were those of Version 8 of the TESLA beam delivery system. The beta functions through the final telescope are shown in Figure 3, and some relevant parameters at the entrance to the telescope and at the interaction point are given in Table 1.

The solenoid field assumed throughout was 4.0 T, and the total length of the solenoid (main field) was assumed to be 9.37 m. With this length, the last quadrupole of the final focus system is just inside the solenoid, i.e. the fringe field is positioned at the entrance to the last quadrupole.

Our approach to the problem is as follows. To study the linear dynamics, we can simply multiply the transfer matrices for the elements in the beam line from the entrance to the final telescope to the interaction point. To see the effect of modifying the beam line (e.g. by inserting a solenoid field or skew quadrupoles), we can calculate the matrix

$$\Delta\mathbf{M} = \mathbf{M}' \cdot \mathbf{M}^{-1}$$

where $\mathbf{M}$ is a matrix representation of the transfer map for the original beam line, and $\mathbf{M}'$ the map for the modified beam line. If we then construct the IP phase space matrix

$$s = \begin{pmatrix} b_x e_x & & & \\ & \frac{e_x}{b_x} & & \\ & & b_y e_y & \\ & & & \frac{e_y}{b_y} \end{pmatrix} \qquad (1)$$

then the effect of modifications to the beam line on the beam size and divergence can be found from

$$s' = \Delta\mathbf{M} \cdot s \cdot \Delta\mathbf{M}^{-1}$$

The horizontal and vertical beam sizes and divergences are just the square roots of the elements on the diagonal of s'. Note that in expression (1) we have used the fact that $a_x^* = a_y^* = 0$.

To perform the calculations, in addition to the standard transfer matrices used in accelerator beam line studies, we require the transfer matrices for a solenoid field, the fringe field, and for a quadrupole with a solenoid field component. These are given in the Appendix.

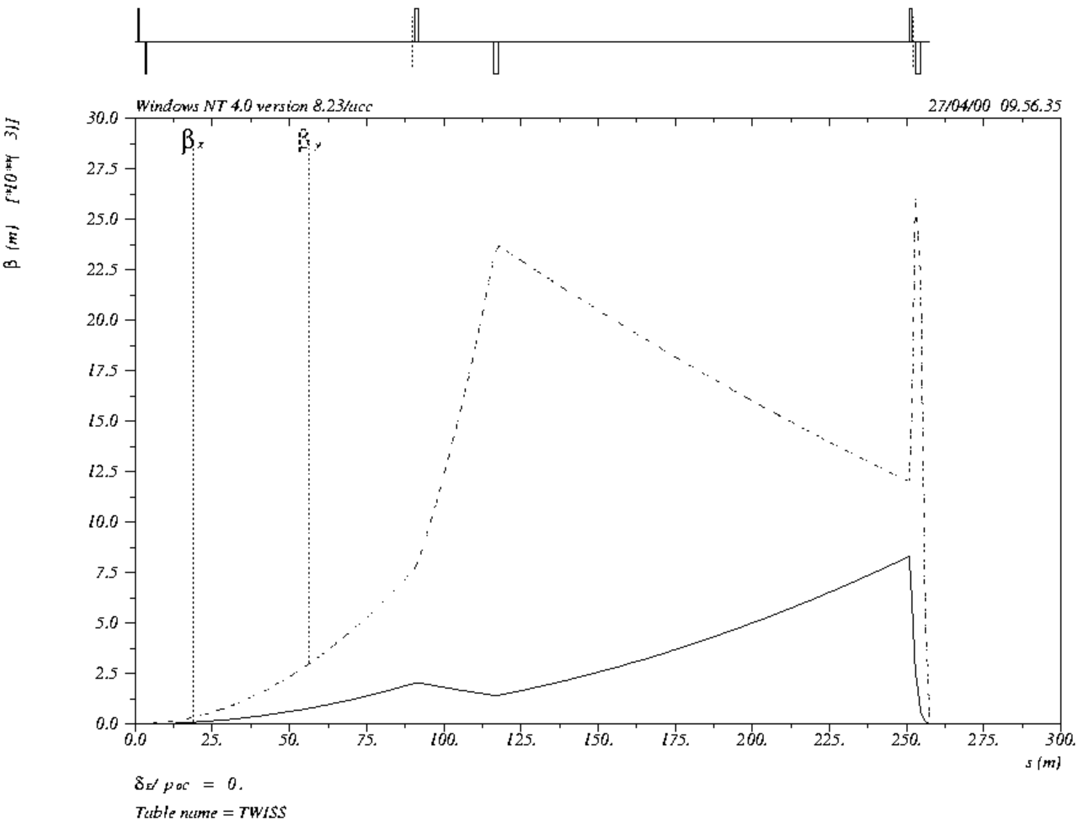

Figure 3
Beta functions through the final telescope, TESLA BDSv8. The vertical broken lines in the magnet layout at the top of the diagram indicate possible locations of the skew quadrupoles for compensating coupling effects of the solenoid.

Parameter	Value at entrance to telescope	Value at interaction point (in absence of solenoid)
Beta functions β_x, β_y /m	163.0, 54.50	0.015, 0.0004
Emittances $\varepsilon_x, \varepsilon_y$ /nm rad	10^{-5}, 3×10^{-8}	10^{-5}, 3×10^{-8}
Beam Size σ_x, σ_y /nm	5.77×10^{4}, 1.83×10^{3}	554, 4.95

Table 1
Values of selected parameters at entrance to final telescope and at interaction point in the TESLA beam delivery system version 8.

4. Correction of Solenoid Effects

Matrix multiplications were performed in Mathematica, and results compared with beam line modelling using DIMAD. In all cases, the results were in close agreement. Figure 4 shows the results obtained for the beam size at the IP with one and two skew quadrupole correctors. For comparison, the beam size with a short solenoid (stopping short of the last quadrupole of the final focus) and no skew correctors is shown. As expected, the coupling effect is small for the short solenoid, since there is effective coupling cancellation between the fringe and main fields. The beam size with a long solenoid and two skew quadrupoles is close to the beam size with no solenoid, and meets the requirements for the target luminosity. This cannot be achieved using a single skew quadrupole.

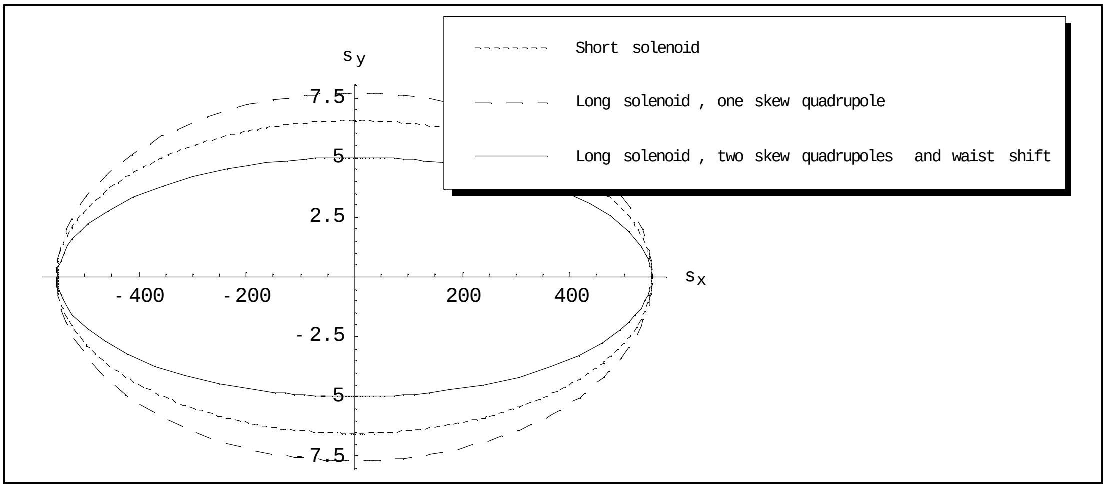

Figure 4
Beam sizes at the interaction point with solenoid field and skew quadrupoles.

	s_x /nm	s_y /nm
No solenoid	553	5.05
Short solenoid, no skew quadrupoles	553	6.53
Long solenoid, no skew quadrupoles	639	963
Long solenoid, one skew quadrupole	553	7.69
Long solenoid, two skew quadrupoles	554	5.66
Long solenoid, two skew quadrupoles and waist shift	551	5.01

Table 2
Beam sizes at the interaction point.

The positions of the skew quadrupoles are as shown in Figure 3. The first is placed at the final doublet. For the calculations with results presented above, it is actually between the two quadrupoles, which would place it inside the cryostat. However, similar results can be obtained with this skew quadrupole placed just upstream of the furthest member of the doublet; in particular, it is still possible to reduce the vertical beam size to 5 nm. The second skew quadrupole was positioned close to the central doublet, but the quality of the correction is insensitive to its precise location.

The strengths of the skew quadrupoles required to achieve the coupling correction are within reasonable limits. Again there is good agreement between strengths determined using Mathematica and using DIMAD; the values obtained using DIMAD are shown in Table 3.

Skew quadrupole	k value /m^{-2}	field gradient /Tm^{-1}
SQ1 at central doublet	2.04×10^{-3}	1.70
SQ2 at final doublet	5.43×10^{-4}	0.453

Table 3
Skew quadrupole settings (with waist shift) required to compensate 4 T solenoid field at IP.

The dependence of vertical beam size on the skew quadrupole settings is of interest, as this will affect the ease with which these magnets can be tuned in practice. Variation of the vertical beam size with skew quadrupole settings is shown in Figure 5.

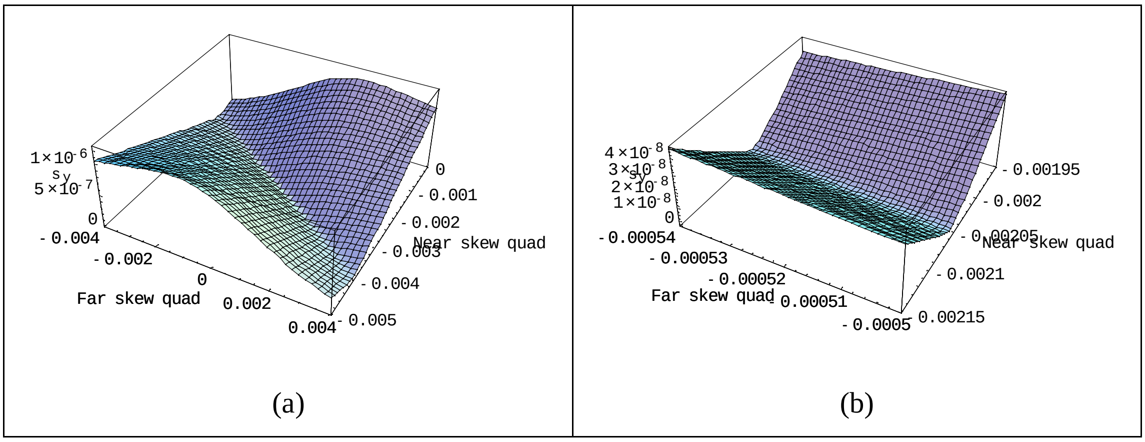

Figure 5
Vertical beam size at the interaction point versus the skew quadrupole settings. (a) shows the vertical beam size over a wide variation of the skew quadrupole strengths; (b) shows the vertical beam size over small variations, approximately ±5%, of the skew quadrupole strengths centred on the optimal values.

The significant aspect of the dependence is the long 'valley', indicating that the two skew quadrupoles are not orthogonal in parameter space. The reason for this becomes clear when we look at the phase advances across the final telescope, shown in Figure 5. The two skew quadrupoles are at approximately the same phase both horizontally and vertically, and separated from the IP by a phase advance of approximately $p/2$, again in both planes. It might appear that to improve the orthogonality, the skew quadrupole furthest from the IP could be moved to the start of the final telescope, where there would then be a phase advance of $p/2$ in both planes between the skew quadrupoles. If this is done, however, we observe that:

- the quality of the correction becomes slightly worse;
- there is no improvement in the shape of the valley in the dependence of vertical beam size on skew quadrupole strengths;
- the required strength of the skew quadrupole at the start of the final telescope increases by three orders of magnitude over the previous case.

An explanation for these observations can be formulated if we look at the transformation induced on the phase space at the IP by the presence of the long 4 T solenoid. In matrix form, this is given by:

$$\Delta\mathbf{M} = \begin{pmatrix} 0.9999 & 8.555\times10^{-6} & 0.01835 & -0.02604 \\ -2.178\times10^{-5} & 0.9999 & 4.422\times10^{-3} & 3.923\times10^{-3} \\ 3.920\times10^{-3} & -0.02605 & 0.9999 & 3.849\times10^{-3} \\ -3.730\times10^{-3} & -0.01836 & -8.554\times10^{-5} & 1.0001 \end{pmatrix} \tag{2}$$

Note that this matrix is expressed in Transport variables, i.e. $(x \quad x' \quad y \quad y')$. We note also that it is not symplectic. In fact,

$$\Delta\mathbf{M}\cdot\mathbf{S}\cdot\Delta\mathbf{M}^T = \begin{pmatrix} 0 & 1 & 0 & 0 \\ -1 & 0 & 0 & 0.004797 \\ 0 & 0 & 0 & 1 \\ 0 & -0.004797 & -1 & 0 \end{pmatrix}$$

where $\mathbf{S}$ is the usual symplectic form. The non-symplecticity arises from the fact that the momentum gmv is not the canonical momentum inside a solenoid, since the transverse components of the magnetic vector potential are large in a solenoid field. Nonetheless, the deviation from symplecticity is small, and for the following qualitative argument, we treat the transformation as though it were symplectic. Thus, we claim we can write a generator that gives a good approximation for the transformation:

$$?M \approx \mathrm{e}^{:f(x,p_x,y,p_y):}$$

Inspection of the matrix representation (2) suggests that the most significant off-diagonal term in f is the $p_x p_y$ term. A skew quadrupole at the IP would introduce a term in xy; with a phase advance of $p/2$ between the skew quadrupole and the IP, the contribution clearly becomes $p_x p_y$, which is exactly the term required to cancel the effects of the solenoid. This explains why the skew quadrupole at the final doublet is so effective at correcting the coupling resulting from the solenoid field. On the other hand, a skew quadrupole positioned at the start of the final telescope, where the phase advance to the IP is p, contributes an xy term to the generator. The corresponding terms in the transformation resulting from the solenoid are an order of magnitude less than the terms corresponding to $p_x p_y$, so a skew quadrupole at this position is expected to be ineffective.

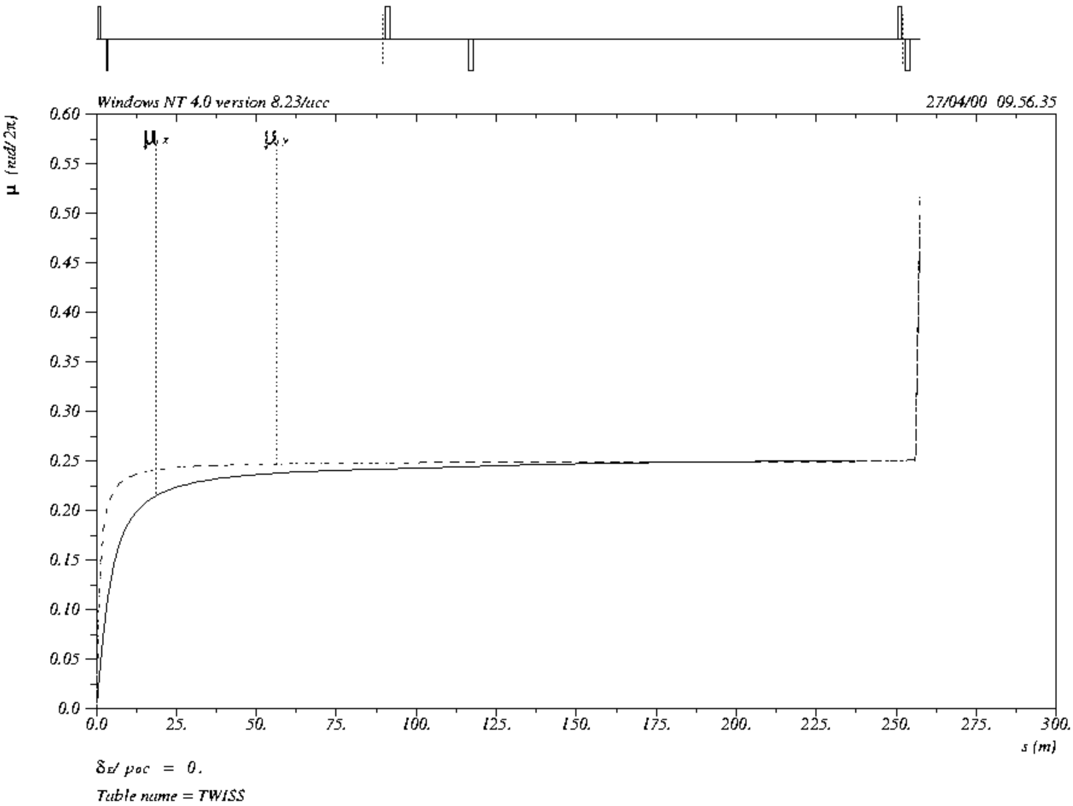

Figure 6
Horizontal and vertical phase advances across the final telescope.

Clearly, great care must be taken in positioning the second skew quadrupole if an effective compensation of the solenoid effects is to be made, while at the same time achieving orthogonality between the two skew quadrupoles in parameter space. We have not carried out a rigorous analysis of the positioning of the skew quadrupoles, but our investigations suggest that orthognality cannot be achieved if these elements are both positioned within the final telescope. Further studies should consider the possibility of placing one skew quadrupole a significant distance upstream, possibly in the chromatic correction section of the beam delivery system. An alternative approach would be to accept the non-orthogonality of the skew quadrupoles, and develop an optimisation algorithm that overcomes the difficulties associated with the long valley in the beam size dependence on skew quadrupole strengths.

Finally, we note that a waist shift of 0.147 mm upstream is required to achieve the minimum vertical beam size of 5 nm. The vertical beam size as a function of longitudinal position is shown in Figure 7, where the nominal interaction point (i.e. the interaction point without solenoid field) is at $z = 0$.

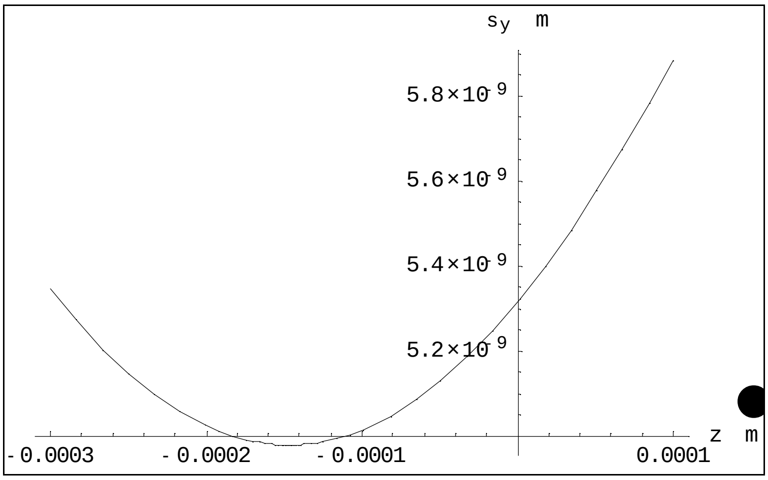

Figure 7
Vertical beam size vs longitudinal position near the nominal interaction point.

5. Sensitivity to Variation in Solenoid Alignment

Of practical interest is the sensitivity of the beam size to variation in the alignment of the solenoid. As initial estimates of the magnitudes of expected effects, we have applied only a very simple model, corresponding to rotations of the solenoid field around horizontal and vertical axes, through the entrance to the solenoid. The last quadrupole, lying inside the solenoid field, is excluded from the rotation of the solenoid. As before, we have only considered linear effects. For this reason, we do not expect that changes in position of the solenoid will significantly affect the beam size after re-optimisation, since we have already shown that the skew quadrupoles are effective at linear correction.

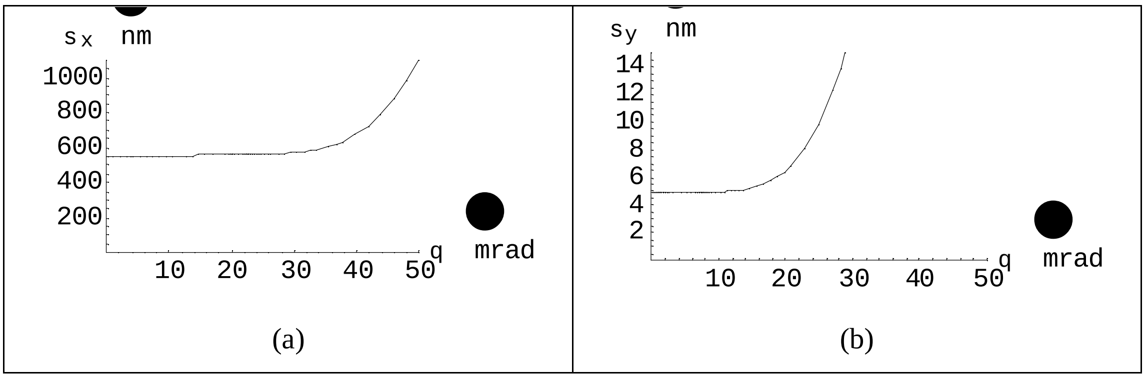

Figure 8
(a) Horizontal and (b) vertical beam sizes at the interaction point, as functions of rotation of the solenoid about a horizontal axis.

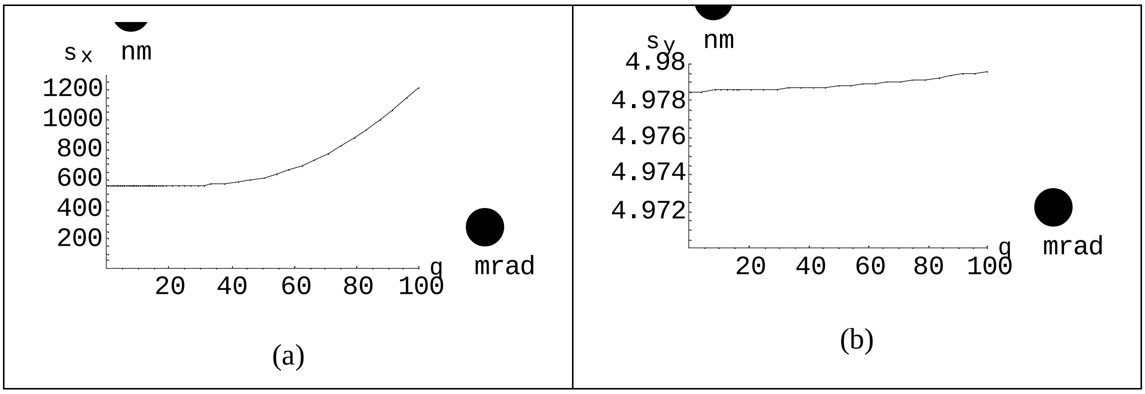

Figure 9
(a) Horizontal and (b) vertical beam sizes at the interaction point, as functions of rotation of the solenoid about a verical axis.

Effects on the beam size of rotating the solenoid about horizontal and vertical axes are shown in Figure 8 and Figure 9 respectively. The graphs show the beam size after re-optimisation of the skew quadrupoles for each angle of rotation. It is found that only small changes to the skew quadrupole strengths are required, up to rotations of about 20 mrad. For example, for a 10 mrad rotation about a horizontal axis, the changes in the skew quadrupole strengths are less than 10%; for a similar rotation about a vertical axis, the changes in strength are much less.

6. Conclusions

The results we have presented suggest that the linear effects of a long solenoid field at the TESLA interaction point can effectively be corrected using two skew quadrupoles in the final focus. There are no significant problems apparent even for a solenoid extending over the final quadrupole, and for a strong 4 T solenoid field. The quality of the correction is insensitive to the precise positioning of the skew quadrupoles, so the closest skew quadrupole to the IP could be moved back upstream of the final doublet. In theory, even with the long solenoid, a vertical beam size of 5 nm can be achieved without great difficulty.

One problem that may require further investigation is the dependence of the vertical beam size on the strengths of the skew quadrupoles. A plot of beam size against the strengths shows a long valley, which could make optimisation of the system difficult in practice. One possible solutions that would merit further investigation is the possibility of moving one of the skew quadrupoles further upstream in the beam delivery system, for example in the chromatic correction section. An alternative approach would be to develop optimisation algorithms that can operate effectively even with the long valley.

We have used a very simple model to investigate the sensitivity of beam size to solenoid alignment. It appears that the skew quadrupole correction is extremely tolerant of rotations in the solenoid field, and can maintain a 5 nm vertical beam size, even with alignments that are much larger than are likely to occur in practice.

Acknowledgements

The author would like to thank Nick Walker for useful discussions and advice, and Olivier Napoly for materials that were extremely helpful in preparing the work reported in this note.

Appendix: Transfer Maps

We give here for reference, and without proof or discussion, the transfer maps used in the work reported, for elements associated with the solenoid field.

Solenoid main field
$$\begin{pmatrix} 1 & \frac{\sin(l_s k_s)}{k_s} & 0 & \frac{1-\cos(l_s k_s)}{k_s} \\ 0 & \cos(l_s k_s) & 0 & \sin(l_s k_s) \\ 0 & -\frac{1-\cos(l_s k_s)}{k_s} & 1 & \frac{\sin(l_s k_s)}{k_s} \\ 0 & -\sin(l_s k_s) & 0 & \cos(l_s k_s) \end{pmatrix}$$

Solenoid fringe field
$$\begin{pmatrix} 1 & 0 & 0 & 0 \\ 0 & 1 & \frac{k_s}{2} & 0 \\ 0 & 0 & 1 & 0 \\ -\frac{k_s}{2} & 0 & 0 & 1 \end{pmatrix}$$

Quadrupole in solenoid [1]

$$\begin{pmatrix} a(b+a)\cos(bl)+b(b-a)\cosh(al) & (b+a)\sin(bl)-(b-a)\sinh(al) & -k_s\left(a\sin(bl)-b\sinh(al)\right) & -k_s\left(\cos(bl)-\cosh(al)\right) \\ k_1\left(-(b+a)\sin(bl)+(b-a)\sinh(al)\right) & b(b+a)\cos(bl)-a(b-a)\cosh(al) & -k_1 k_s\left(\cos(bl)-\cosh(al)\right) & k_s\left(b\sin(bl)+a\sinh(al)\right) \\ k_1 k_s\left(\frac{\sinh(al)}{a}-\frac{\sin(bl)}{b}\right) & k_s\left(\cos(bl)-\cosh(al)\right) & -a(b-a)\cos(bl)+b(b+a)\cosh(al) & (b-a)\sin(bl)+(b+a)\sinh(al) \\ -k_1 k_s\left(\cos(bl)-\cosh(al)\right) & -k_s\left(b\sin(bl)+a\sinh(al)\right) & k_1\left((b-a)\sin(bl)+(b+a)\sinh(al)\right) & b(b-a)\cos(bl)+a(b+a)\cosh(al) \end{pmatrix}$$

where

quadrupole strength $k_1 = \frac{1}{B r}\frac{\partial B_y}{\partial x}$;

solenoid strength $k_s = \frac{1}{B r} B_s$, with solenoid main field strength B_s, and length l_s;

$$a = \sqrt{\frac{-k_s^2 + \sqrt{k_s^4 + 4k_1^2}}{2}} \qquad b = k_1\sqrt{\frac{2}{-k_s^2 + \sqrt{k_s^4 + 4k_1^2}}}$$

References

[1] O. Napoly, private communication, March 2000. The transfer matrix for a combined quadrupole and solenoid field was calculated by R. Helm, and later by S. Fartouhk, and has been incorporated in DIMAD.